PHYSICAL REVIEW B **87**, 064302 (2013)

Effect of pressure, temperature, fluorine doping, and rare earth elements on the phonon density of states of *L*FeAsO studied by nuclear inelastic scattering

I. Sergueev,[1,2,3,*] R. P. Hermann,[2,4] D. Bessas,[2,4,1] U. Pelzer,[1] M. Angst,[2,5] W. Schweika,[2,6]
M. A. McGuire,[7] A. S. Sefat,[7] B. C. Sales,[7] D. Mandrus,[7,8] and R. Rüffer[1]

[1]*European Synchrotron Radiation Facility (ESRF), P.O. Box 220, F-38043 Grenoble, France*
[2]*Jülich Center for Neutron Science JCNS and Peter Grünberg Institut PGI, JARA-FIT, Forschungszentrum Jülich GmbH, D-52425 Jülich, Germany*
[3]*Deutsches Elektronen-Synchrotron, D-22607 Hamburg, Germany*
[4]*Faculté des Sciences, Université de Liège, B-4000 Liège, Belgium*
[5]*Experimental Physics IVC, RWTH Aachen University, D-52056 Aachen, Germany*
[6]*European Spallation Source AB, S-22100 Lund, Sweden*
[7]*Materials Science and Technology Division, Oak Ridge National Laboratory, Oak Ridge, Tennessee 37831, USA*
[8]*Department of Materials Science and Engineering, The University of Tennessee, Knoxville, Tennessee 37996, USA*
(Received 7 January 2013; published 25 February 2013)

We have performed systematic studies of the lattice dynamics in *L*FeAsO (L = La, Ce, Pr, Nd, Sm) in the parent and in the ∼10% F-doped compounds as a function of pressure and temperature. We have found that the modifications in the partial Fe density of phonon states are mainly governed by the Fe-As bond length. The change of this bond length explains the change of the Fe density of phonon states above 25 meV. We further observe anomalies in the behavior of the phonon mode near 16 meV. In the parent phase, this mode softens anomalously upon cooling through the structural phase transition. Upon F doping, this mode hardens indicating a strong electron-phonon coupling. This suggests that the corresponding phonons play an important role in the competition between superconductivity and magnetism in these materials.

DOI: 10.1103/PhysRevB.87.064302 PACS number(s): 63.20.dd, 74.70.Xa

I. INTRODUCTION

The discovery of high-temperature iron-based superconductors[1] has attracted intensive theoretical and experimental research efforts.[2–4] All the recently discovered iron-based superconductors have a layered structure with planes of iron linked by tetrahedrally coordinating As or Se/Te. In the compounds with a ZrCuSiAs type structure (1111 family) the Fe-As layers are separated by layers of *L*O, with *L* denoting a rare earth element. The parent compounds experience both a magnetic and a structural phase transition between 130 and 180 K. Both transitions are suppressed with the subsequent appearance of superconductivity by electron doping via either partial substitution of oxygen by fluorine or oxygen deficiency achieved via high pressure synthesis. The superconductive temperature T_c for the optimally doped compounds of the 1111 family reaches 55 K, e.g., in $SmFeAsO_{0.85}$ and in $SmFeAsO_{0.9}F_{0.1}$, which is the highest T_c for iron based superconductors. Application of high pressure is another way to induce superconductivity in the iron pnictides of the 122 family, RFe_2As_2,[5] where indications of bulk or filamentary superconductivity have been observed under certain pressure conditions for R = Ca, Sr, Ba, Eu. In contrast, the high pressure induced superconductivity in the 1111 family depends on the compound. It was observed[6] for LaFeAsO, but was not observed[7] for CeFeAsO.

The complex phase diagram of the iron pnictides, which includes magnetic, structural, and superconductive phase transitions, is an indication of the complex coupling between electronic, magnetic, and structural properties, which also should affect the lattice dynamics. First-principle calculations show that the magnitude of the electron-phonon coupling as well as phonon properties crucially depend on the presence and the magnitude of the magnetic moment at the iron site.[8] The correct theoretical description of the experimentally observed phonon spectra requires artificial softening of the force constants[9] or spin-polarized (magnetic) calculations even for doped compounds, where the magnetic phase is suppressed.[10,11] An experimental test of the magnetoelastic and electron-phonon coupling can be obtained by the investigation of the lattice-dynamics response to changes of external parameters such as temperature and pressure. In particular, the comparison of the doping and pressure effect is important since both of them potentially can lead to superconductivity.

Experimental studies of the lattice dynamics in compounds of the 1111 family are complicated because of the lack of good quality single crystals. Most of the studies performed by Raman scattering,[12–17] inelastic x-ray,[9,18–21] neutron,[22–24] and nuclear inelastic scattering[25] (NIS) reported minor changes of the lattice dynamics with temperature or doping. However, investigations under high pressure are absent for the 1111 family of iron based superconductors.

In this paper, we report a systematic study of the lattice dynamics in the 1111 family of iron based superconductors (iron pnictides) carried out by nuclear inelastic scattering with sub-meV energy resolution. The partial Fe density of phonon states (DPS) has been obtained for several *L*FeAsO compounds with the substitution of rare earth (L = La, Ce, Pr, Nd, Sm). Three of these compounds (L = La, Nd, Sm) have been investigated in the parent and optimally doped states as a function of temperature, $T < 300$ K. The lattice dynamics under high pressure, up to 5 GPa, has been investigated for La and Nd parent compounds. In addition, the partial Sm DPS has been studied in the parent and doped SmFeAsO.

This systematic study reveals a universal relation between structure and lattice dynamics, which describes the position of

TABLE I. Refined lattice constants, As positional parameter, and unit cell volume from the Rietveld refinements of the x-ray powder diffraction data. The *P4/nmm* space group was used for the refinement. ∗ denotes data from Ref. 30. V_{FeAs} is calculated according to the equation in Sec. IV C and shown in Fig. 1.

Composition	a (Å)	c (Å)	z_{As}	V (Å^3)	V_{FeAs} (Å^3)
LaFeAsO	4.0321(1)	8.7380(4)	0.6533(4)	142.06(1)	43.55(6)
$LaFeAsO_{0.9}F_{0.1}$	4.0318(2)	8.7235(4)	0.6547(6)	141.80(2)	43.87(9)
CeFeAsO	4.0025(3)	8.6441(4)	0.6544*	138.48(2)	42.76
PrFeAsO	3.9862(2)	8.6184(5)	0.6561*	136.94(2)	42.75
NdFeAsO	3.9665(2)	8.5761(5)	0.6569(4)	134.93(2)	42.34(6)
$NdFeAsO_{0.9}F_{0.1}$	3.9604(4)	8.5520(10)		134.14(3)	
SmFeAsO	3.9391(1)	8.4995(3)	0.6615(3)	131.88(1)	42.60(5)
$SmFeAsO_{0.88}F_{0.12}$	3.9311(1)	8.4733(3)		130.94(1)	

the peaks in the Fe DPS above 25 meV. In contrast, anomalies in the temperature behavior of the phonon modes near 16 meV were found for both parent and doped compounds. A 5% relative hardening of the peak position is observed in the doped compounds. The anharmonic phonon behavior at this energy is likely a sign of the electron- or spin-phonon coupling. Thus, the phonons at 16 meV can play an important role in the competition between magnetism and superconductivity in iron pnictides.

II. SAMPLE PREPARATION AND CHARACTERIZATION

Polycrystalline samples of LaFeAsO, CeFeAsO, PrFeAsO, NdFeAsO, and SmFeAsO were prepared by the procedure described elsewhere.[26–28] La, Nd, and Sm compounds were prepared in the parent and the fluorine doped state. Rare-earth fluorides were used as the fluorine source. The nominal fluorine concentration was 0.1 for the La and Nd compounds and 0.12 for the Sm compound. The La, Nd, and Sm samples were enriched by ^{57}Fe to 90%. In addition, the Sm parent and doped compounds were enriched by ^{149}Sm to ∼50%.

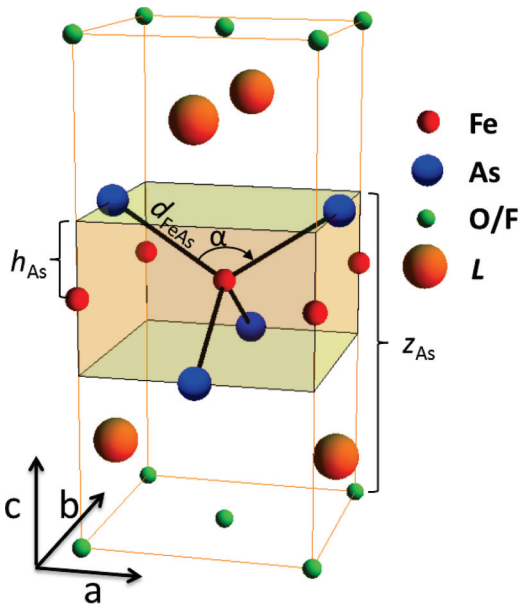

FIG. 1. (Color online) Schematic diagram of the crystal structure of *L*FeAsO. The shaded area depicts Fe-As subvolume of the unit cell with volume V_{FeAs}.

The structure and crystallographic purity of the samples were characterized by powder x-ray diffraction using MoKα radiation in a calibrated Huber G670 diffractometer. The data were Rietveld refined using FULLPROF.[29] Refined lattice parameters and atomic positions of the As atom in the unit cell (space group *P4/nmm*) at 295 K shown in Table I are consistent with the results of other studies of similar compounds.[30,31] The superconductive transition temperatures were identified in the doped samples by magnetic susceptibility measurements as $T_c = 28$, 48, and 51 K for La, Nd, and Sm compounds, respectively.

The chemical purity of the compounds was further checked using iron-57 Mössbauer spectroscopy measurements performed at room temperature. The data reveals no impurities for all samples except $SmFeAsO_{0.88}F_{0.12}$. In the latter, <10% of an iron based impurity were identified.

III. EXPERIMENTAL SETUP AND PROCEDURE

The nuclear inelastic scattering experiments were performed at the nuclear resonance beamlines[32] ID18 and ID22N of the European Synchrotron Radiation Facility operated in 16-bunch mode of the storage ring. The measurements utilizing the nuclear resonance of the ^{57}Fe at 14.413 keV were performed with an inline high resolution monochromator providing an energy bandwidth of 0.7–0.8 meV FWHM (full width at half maximum) depending on the current in the storage ring. The measurements with the nuclear resonance of ^{149}Sm at 22.502 keV[33] were performed using an inline channel-cut high resolution monochromator[34] with an energy bandwidth of 1.1 meV.

The temperature-dependent measurements between 20 and 300 K were performed with the samples inserted into a closed cycle cryostat. The measurements under high pressures were performed at room temperature using polycrystalline samples loaded into Be gaskets with a ∼100 μm hole together with small ruby chips used as a pressure marker. The pressure transmitting medium was a 4:1 methanol:ethanol mixture providing hydrostatic conditions in the studied pressure range. The gaskets were mounted into panoramic-type diamond anvil cells.[35] The beam after the high resolution monochromator was focused to a spot of 10 × 20 μm^2 using Kirkpatrick-Baez mirrors.

Typical NIS spectra measured using the ^{57}Fe and ^{149}Sm nuclear resonances are shown in Fig. 2 along with the

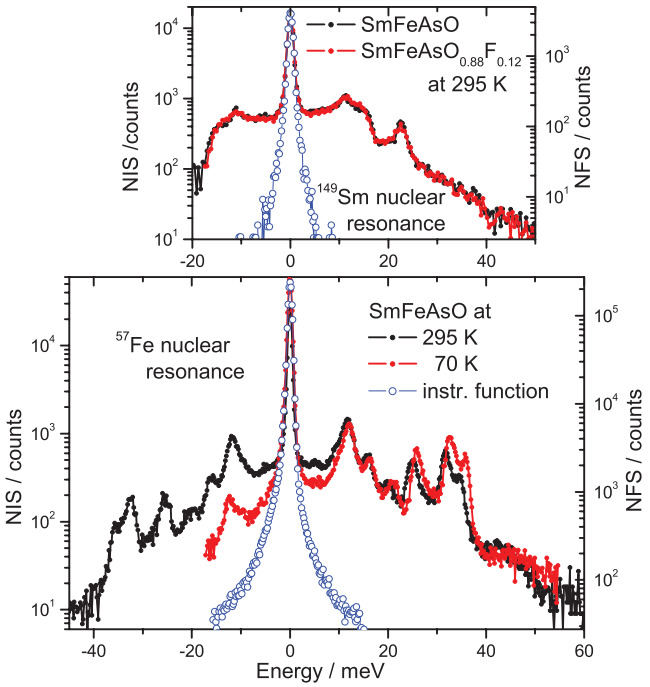

FIG. 2. (Color online) ^{149}Sm (top) and ^{57}Fe (bottom) nuclear inelastic scattering (NIS) spectra of $SmFeAsO_{1-x}F_x$. The blue open circles represent the instrumental functions measured by nuclear forward scattering (NFS) (right scale).

instrumental functions simultaneously measured by the time integrated nuclear forward scattering. The typical duration of the measurements was ∼1–2 hours for the ^{57}Fe NIS spectra at ambient pressure and ∼6 hours for the ^{57}Fe NIS spectra at high pressures and for the ^{149}Sm NIS spectra.

The partial densities of phonon states were evaluated from the NIS spectra using the procedure described in Ref. 36. No deconvolution with the instrumental function was applied, so that the statistical noise in the DPS reproduces that in the NIS spectra. The area of all obtained DPSs deviates by less than 2% from unity as must be obtained in the ideal procedure.

For this work it was extremely important to find the energy shift of specific peaks in the DPS due to changes of external conditions. In order to define such shifts in a precise way we have used the following procedure. The DPS with the best statistics was used as a theoretical function $D(E)$ via linear interpolation of the data. All other DPSs were fitted in the regions of the peak of interest by the function $\beta \cdot D[(1+\alpha)\cdot E]$, where α and β are fit parameters. The parameter α gives the relative shift of the peak position $\alpha = \Delta E/E$. The parameter β, which is equal to $1+\alpha$ for the ideal DPSs due to the normalization of the DPS area to unity, is introduced in order to account for possible statistical noise. The results were checked for consistency using different DPSs as a reference theoretical function. The advantage of this procedure, as compared to the calculation of the center of mass of the peak, is that it does not depend on the shape of the region of interest chosen for the peak under consideration. The assumption which defines the accuracy of this procedure is that the shape of the peak does not vary with external conditions, which is essentially verified in this study.

The main contribution to the experimental error of the energy scale is due to the change of the thermal conditions of the monochromator with a characteristic time scale of six hours. This error is estimated as $\delta(\Delta E/E) = 0.5\%$ from a set of independent measurements on the same sample. However, this error is not taken into account when considering the relative positions of the different peaks in the DPS which is important for Fig. 9 in Sec. IV D and the related discussion.

IV. EXPERIMENTAL RESULTS

A. Parent compounds at ambient conditions

The partial Fe and Sm DPSs of SmFeAsO obtained at 295 K are shown in Fig. 3. The scales of the Fe and Sm DPSs are presented with the atomic mass ratio $m_{Sm}/m_{Fe} = 149/57$ which leads to the same Debye level of both DPSs.[37]

The phonons in Fig. 3 can be separated into three parts. The low energy part below 17 meV, where vibrations of Fe and Sm are quite similar and correspond mainly to the acoustical phonon branches, includes two peaks at 12 and 16 meV observed for both atoms. The intermediate energy part between 20 and 27 meV includes a Sm peak at 23 meV and two Fe peaks at 20 and 25 meV. Here, the Sm and Fe vibrations are well decoupled. The high energy part above 29 meV consists of the strong Fe peak at 32 meV and a pronounced shoulder of this peak at 33–35 meV.

Our data are consistent with a generalized DPS obtained by inelastic x-ray scattering measurements[21] on the same compound with good coincidence of the peak positions as seen from Fig. 3. Also, the shape of the Fe DPS is similar to that measured by NIS in other iron based superconductors of the 1111 and 122 families.[25,38–40] Comparison of the Sm and Fe DPSs with Raman data[14,17] measured on SmFeAsO allows us to identify the peak at 32 meV with a stretching A_{2u} mode, the shoulder at 34 meV, and the peak at 16 meV with E_g modes.

The Fe DPSs measured at 295 K in all studied compounds are shown in the Fig. 4. The characteristic parameters calculated from the DPS, namely the Lamb-Mössbauer factor

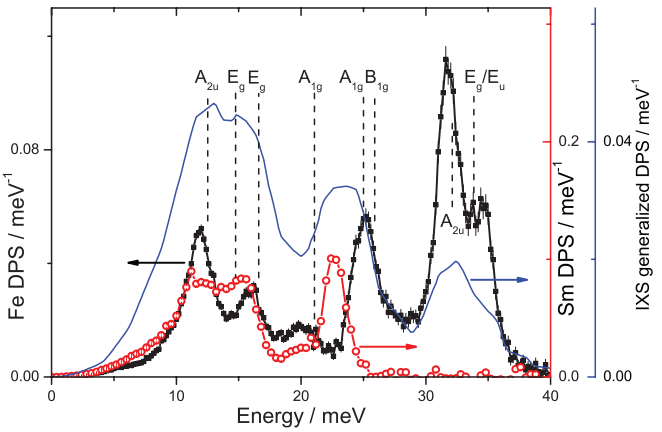

FIG. 3. (Color online) Partial Fe (black, left scale) and Sm (red, right scale) DPS of SmFeAsO at 295 K. The left and right scales ratio corresponds to the mass ratio of Sm and Fe atoms. In addition, the generalized DPS (blue, right scale) of the same compound obtained by inelastic x-ray scattering (IXS) is shown.[21] The vertical lines denote the positions of the Raman peaks on the same compound.[14,17]

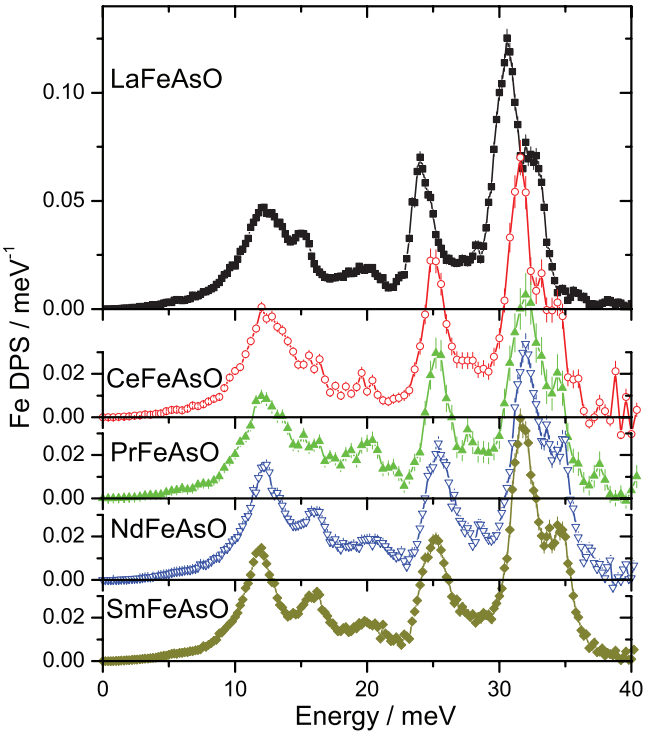

FIG. 4. (Color online) Fe DPS in several compounds of the 1111 family of iron based superconductors measured at 295 K.

f_{LM}, the atomic displacement parameter U_{eq}, and the Debye temperature ϑ_D calculated from f_{LM}, the mean force constant F, and the averaged Debye sound velocity $\langle v_D \rangle$ calculated from the acoustical part of the DPS, are presented in the Table II.

The DPSs for all compounds are similar and include the same set of peaks. However, the positions of the peaks vary between compounds. The Fe DPSs of La, Nd, and Sm compounds, measured with good statistics, are compared in Fig. 5, where the energy is scaled for the Nd compound by 0.994 and for the La compound by 1.040 in order to match the same position of the 32 meV peak of the Sm compound. The inverse scaling coefficients are applied to the DPS scale in order to keep the area equal to unity.

The same scaling coefficient describes the shift of the 20, 25, and 32 meV peaks in these compounds, which signifies the same influence of the structural changes on these peaks. However, the 12 meV peak does not follow the same trend,

TABLE II. The Lamb-Mössbauer factors f_{LM}, atomic displacement parameters U_{eq} obtained from f_{LM}, Debye temperatures ϑ_D, mean force constants F, and mean sound velocities $\langle v_D \rangle$ in LFeAsO at 295 K.

LFeAsO	Element	f_{LM}	U_{eq} (pm^2)	ϑ_D (K)	F (N/m)	$\langle v_D \rangle$ (km/s)
La	Fe	0.68(1)	72(3)	365(5)	137(1)	2.75(7)
Ce	Fe	0.69(1)	70(3)	377(5)	145(2)	2.80(10)
Pr	Fe	0.69(1)	70(3)	376(5)	145(2)	2.80(10)
Nd	Fe	0.70(1)	67(3)	381(5)	148(1)	2.77(7)
Sm	Fe	0.70(1)	67(3)	382(5)	148(1)	2.73(7)
Sm	Sm	0.48(1)	56(2)	237(3)	149(5)	2.58(10)

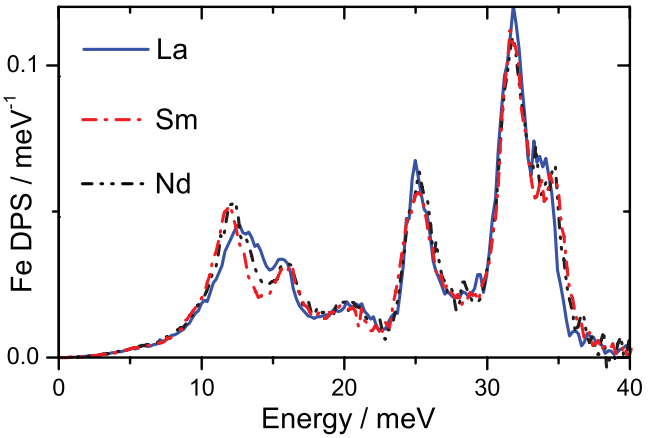

FIG. 5. (Color online) Comparison of Fe DPSs in LaFeAsO, SmFeAsO, and NdFeAsO measured at 295 K. The energy for the Nd compound is scaled by 0.994 and for the La compound by 1.040 in order to have the same position of the 32 meV peak for all DPSs. The same scaling coefficients are applied to the DPS scale to keep the area equal unity.

particularly for the La compound. This can be explained by the coupling of the Fe and rare earth vibrations around 12 meV and, therefore, by the dependence of the peak position on the rare earth atomic mass and radius. The decrease of the rare earth mass from Sm to La leads to a hardening of the peak. The similar hardening of the low energy part of the generalized DPS with the decrease of the rare earth mass was observed in Ref. 24.

A deviation from the general scaling is observed for the 16 meV peak and 34 meV shoulder. Both these features becomes softer for La as compared to Nd and Sm compounds. The vibrations at these energies correspond to the E_g modes. Note that such an effect is much more pronounced for the 34 meV shoulder.

B. High pressure study

Additional information about the correlations between the lattice dynamics and the structure was obtained from the high-pressure studies. The measurements were performed at room temperature at 2.3 and 5.5 GPa for LaFeAsO and at 2.5 and 4.9 GPa for NdFeAsO.

The Fe DPSs of LaFeAsO at 5.5 GPa and NdFeAsO at 4.9 GPa are shown in Fig. 6 together with DPSs measured at ambient pressure, where scales are adjusted to have the same position of the 32 meV peak. The application of pressure leads to the expected hardening. This hardening, however, does not change the overall shape of the DPS, and is described by a unique scaling coefficient for the entire DPS. The relative hardening with pressure is described by $\Delta E/E = 0.017(1) \cdot P/\text{GPa}$ for LaFeAsO and by $\Delta E/E = 0.011 \cdot P/\text{GPa}$ for NdFeAsO, where P denotes the pressure in GPa. The response of the La compound to the applied pressure is larger by 50% than the one in the Nd compound. This effect correlates with the difference in the pressure driven volume contraction for these compounds: $\Delta V/V = -P/B_0$ where B_0 is the bulk modulus which is equal to 70 GPa for $LaFeAsO_{0.95}F_{0.05}$ and 102 GPa for $NdFeAsO_{0.88}F_{0.12}$ as follows from high-pressure diffraction

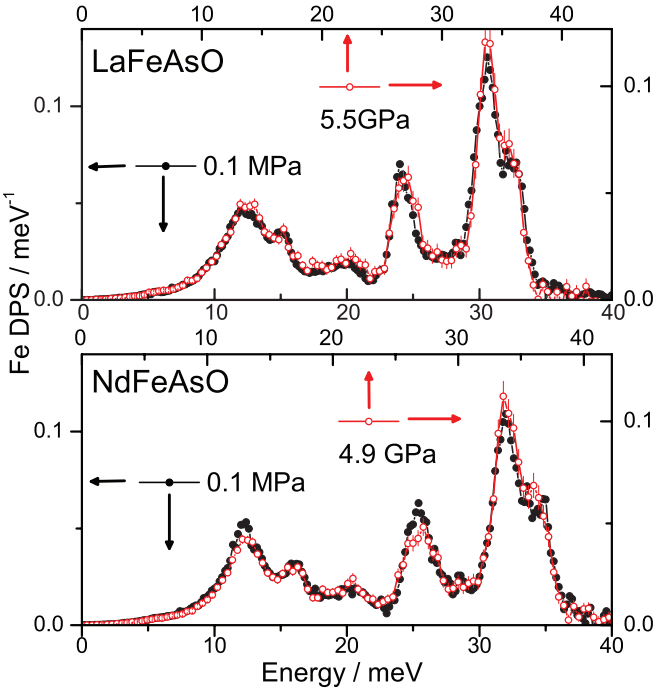

FIG. 6. (Color online) Fe DPS of LaFeAsO (top) and NdFeAsO (bottom) measured at ambient and high pressures at 295 K. The left and bottom scales correspond to the ambient pressure, the right and top scales corresponds to the high pressure measurement.

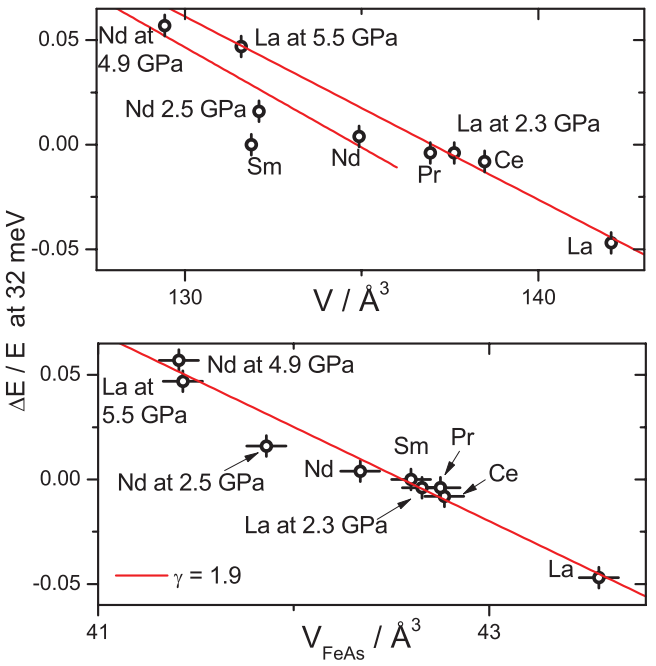

FIG. 7. (Color online) Dependence of the relative 32 meV peak position on the unit cell volume (top) and on the FeAs part of the unit cell volume (bottom) at 295 K. The red lines show the linear fits for the data on the same compounds measured at different pressures (top) and for all data points (bottom).

studies.[41,42] The doping has a minor effect on B_0 (less than 6%),[41,43] therefore these values of B_0 we use to characterize the parent compounds. The hardening of the lattice vibrations with pressure is typically characterized by the Grüneisen parameter $\gamma = -(\Delta E/E)/(\Delta V/V)$. Using bulk moduli from diffraction studies one obtains $\gamma = 1.2$ and 1.1 for La and Nd compounds. These values of γ are somewhat smaller than the expected $\gamma \simeq 2$ for metallic solids. At the same time, the Grüneisen parameters observed in our study are between the values of 1.4–1.8 obtained for $BaFe_2As_2$[38] and 0.9–1.0 obtained for FeSe[44] observed in similar pressure ranges.

C. General scaling of the DPS

The application of pressure as well as the substitution with heavier rare earth elements leads to the contraction of the unit cell and to the corresponding hardening of the Fe DPS. Thus, it is possible to compare the influence of chemical and real pressures on the DPSs by the comparison of the position of the 32 meV peak for different conditions. The other peaks of the DPS follows the similar tendency as shown in the previous sections. The relative shift $\Delta E/E$ of this peak as compared with that in SmFeAsO at ambient conditions is shown in Fig. 7(a) as a function of the unit-cell volume. The data does not follow one curve. In particular, the position of the peak is almost the same for the Sm and Nd compounds at ambient conditions and for the La compound at 2.3 GPa. However, the unit cell volumes for these samples are different. This nonscaling can be accounted for by assuming that the position of the peaks in the Fe DPS depends only on the volume of the Fe-As part of the unit cell which can be defined as $V_{FeAs} = 2 \cdot h_{As} \cdot a^2$, where h_{As} is the height of the As atom above the Fe plane as depicted in Fig. 1, $h_{As} = (z_{As} - 0.5)c$. The a and c lattice parameters and As atomic position z_{As} are presented in Table I. The relative shift of the 32 meV peak as a function of V_{FeAs} is shown in Fig. 7(b). With this choice of the effective volume the data for compounds with different rare earths obey the same linear dependence, with a Grüneisen parameter $\gamma = 1.9$, using V_{FeAs} as the volume parameter. The calculation of the V_{FeAs} for the high pressure data is more difficult since there is no published data on the z_{As} as a function of pressure for NdFeAsO and LaFeAsO. However, several studies[45,46] show that the As-Fe-As bond angles stays almost constant in the pressure range below 10 GPa. Therefore, we assume that the V_{FeAs} decreases proportionally to the cube of the a-lattice parameter reported in Refs. 41, 42, and 45. Obtained in this way the relative shift of the 32 meV peak as a function of V_{FeAs} is shown in Fig. 7(b) and follows the same linear dependence as the ambient pressure data.

The linear dependence of the Fe DPS hardening on the Fe-As volume is, in fact, equivalent to the linear dependence on the Fe-As bond length. The Fe-As volume can be represented as $V_{FeAs} = 8 \cdot d_{FeAs}^3 \cdot \sin^2\alpha/2 \cdot \cos\alpha/2$, where d_{FeAs} is the Fe-As bond length and α is the Fe-As-Fe bond angle as shown in Fig. 1. In 1111 compounds, α is very close to the regular tetrahedron angle value 109.47°, where $dV_{FeAs}/d\alpha = 0$. Thus, around this angle the relative change of the volume is $\Delta V_{FeAs}/V_{FeAs} \simeq 3\Delta d_{FeAs}/d_{FeAs} - 3\Delta\alpha^2/4 \simeq 3\Delta d_{FeAs}/d_{FeAs}$. Consequently, the hardening of the Fe DPS is proportional to the change of the Fe-As bond length $\Delta E/E = -5.7\Delta d_{FeAs}/d_{FeAs}$.

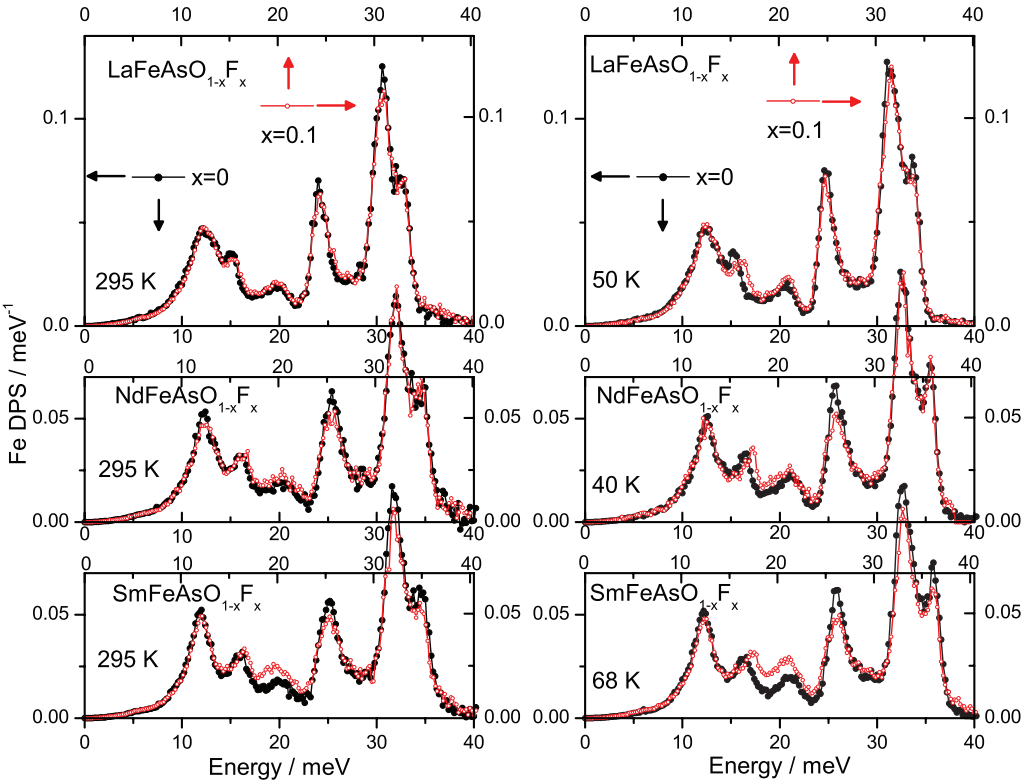

FIG. 8. (Color online) Fe DPS of parent (black, filled circles) and fluorine doped (red, open circles) La-, Nd-, and SmFeAsO measured at 295 K (left side) and at low temperatures (right side). For each graph the bottom and left scales correspond to the parent, and the top and right scales correspond to the doped compound.

D. Temperature and doping dependence

The Fe DPSs in the parent and fluorine doped LaFeAsO, NdFeAsO, and SmFeAsO measured at room temperature and at low temperature are compared in Fig. 8. The doping does not produce significant changes in the Fe DPS at room temperature. The small hardening of the entire DPS by $\Delta E/E \sim 0.005-0.01$ observed for the doped compounds corresponds to the small contraction of the lattice as seen from Table I. In contrast, the comparison of the Fe DPS measured at low temperatures clearly shows the difference in the phonon peak at ~16 meV between doped and parent compounds. For all three compounds this peak is harder by ~0.7 meV in the doped samples.

The temperature dependence of the Fe DPS was investigated at several temperatures below 295 K for the parent and doped Nd and Sm compounds. No big difference in the DPS shape was observed. In particular, there is no difference in the DPSs of the doped compounds across superconductive transition. The relative shift $\Delta E/E$ of the phonon peak at ~32 meV is shown in Fig. 9(a) as compared with the position of this peak in the parent compound at 295 K. For all samples this peak softens continuously with increasing temperature without pronounced features at the superconductive or structural phase transition temperatures. Between lowest and room temperature the peak softens by $\Delta E/E \simeq 0.03$ or $\Delta E \simeq 1$ meV. A similar softening was observed in Ref. 38 for $BaFe_2As_2$ with, however, a jump of the peak position at the structural phase transition.

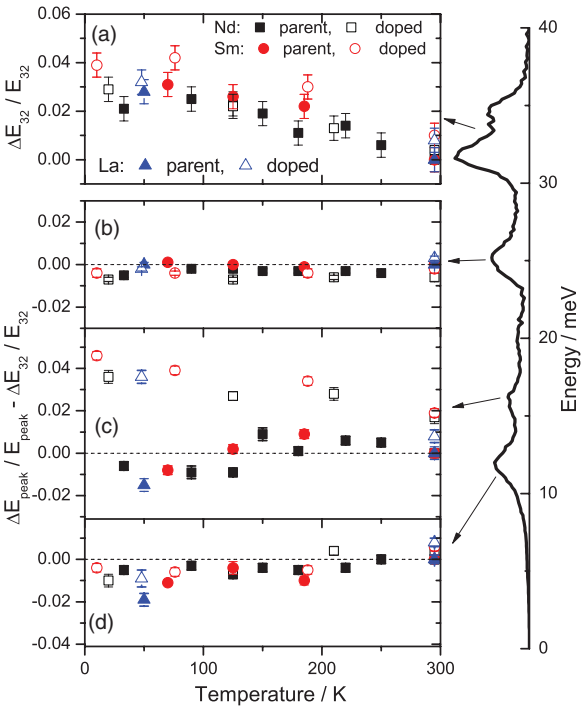

FIG. 9. (Color online) (a) Temperature dependence of the position of the peak at 32 meV for La (blue), Nd (black), and Sm (red) parent (filled symbols) and doped (open symbols) compounds. (b)–(d) Temperature dependence of the peaks at ~25, ~16, and ~12 meV as compared with the position of the ~32 meV peak.

The relative shift $\Delta E/E - \Delta E_{32}/E_{32}$ of the ∼12, ∼16, and ∼25 meV peaks is shown in Figs. 9(b)–9(d). The error of such shift is almost independent of systematic errors and is thus defined only by the statistics of the experiment. If the entire DPS changes proportionally with the same $\Delta E/E$, as it occurs for the measurements under high pressure, then such a relative shift has to be equal to zero. Figure 9(b) shows that the ∼25 meV peak behaves similar to the ∼32 meV peak. Neither doping nor temperature change the relative position of the peak in the Fe DPS. The same tendency is observed for the ∼12 meV peak as seen in Fig. 9(d). The position of the peak is not affected by the doping. A slight increase is observed with the temperature increase which means that the softening of this peak with temperature is less than that of the ∼32 meV peak.

In contrast to the above, a pronounced effect of doping and temperature is well visible for the ∼16 meV peak in Fig. 9(c). The doping leads to a hardening of the ∼16 meV peak at low temperatures by ∼0.7 meV. Upon increasing the temperature the peak in the doped compounds shows enhanced softening as compared to the softening of the 32 meV peak. On the other hand, the position of this peak in the parent compound shows slight hardening at the phase transitions. The different temperature behavior of the ∼16 meV peak in the parent and doped compounds results in a shift less than 0.3 meV of this peak due to the doping at room temperature.

In addition to the modification of the 16 meV peak position, the doping leads to a change of the peak heights. The 20 meV peak is enhanced whereas the magnitude of the 25 and 32 meV peaks decreases. This effect is strong for the Sm compound, weak for the Nd compound, and almost absent for the La compound. This effect does not change with temperature. The increase of the ∼20 meV peak corresponds to the increase of the Fe vibration amplitude at this energy. However, the presence of this effect mainly in the doped Sm compound could be related to the presence of the impurity in the sample.

The effect of the doping on the rare earth vibrations was studied for the Sm atom in $SmFeAsO_{1-x}F_x$. The Sm DPSs measured in the parent and doped compounds at 295 K are shown in Fig. 10. Because the doping modifies the SmO layer, one would expect a pronounced modification of the Sm vibrations. However, the difference in the DPS is quite small, as is seen in Fig. 10 and in the raw data in Fig. 2. The peak at 22.7 meV with FWHM of 2.2 meV upon doping becomes 30% broader and softens by 0.15 meV. A more pronounced effect is observed for the 15 meV peak, which upon doping softens by 1 meV. Taking into account that the peak at 16 meV in Fe DPS becomes harder upon doping, the gap between Sm and Fe phonon peaks at ∼16 meV (see Fig. 3) increases from 0.5 meV in the parent compound to 1.4 meV in the doped compound.

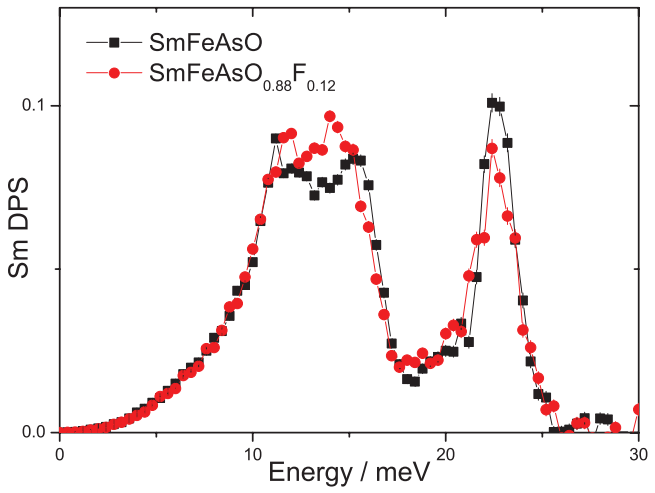

FIG. 10. (Color online) Sm DPS of the parent and doped SmFeAsO measured at 295 K.

V. DISCUSSION

This systematic study of the Fe DPS as a function of the rare earth replacement, doping, and pressure and temperature variations allows us to draw several conclusions. The total shape of the DPS changes only slightly with all studied modifications. The main effect is the scaling of the entire DPS in energy proportional to the characteristic structure changes.

The most pronounced peaks in the Fe DPS (see Fig. 3) are at 25 and 32 meV. The relative positions of these peaks are always the same, which leads to the conclusion that the positions of these peaks is defined by the same structure parameter, which is the Fe-As bond length or, equivalently, the volume of the Fe-As layer. The variation of the relative positions of these peaks with pressure and with rare earth replacement can be described by a simple relation, $\Delta E/E = -1.9\Delta V_{FeAs}/V_{FeAs} = -5.7\Delta d_{FeAs}/d_{FeAs}$. A possible coupling[10,47] of phonons at these energies with electrons or with spin fluctuations is only indirect and occurs via change of the distance between atoms in the Fe-As layer. Note that the variation of the Fe-As part of the unit cell volume is not always proportional to the variation of the entire volume of the unit cell. Therefore, using the unit cell volume instead of the Fe-As layer volume in the analysis of the lattice dynamics via a Grüneisen parameter might lead to wrong conclusions about the mechanisms describing the behavior of the 25 and 32 meV peaks. As such, the difference of the isobaric and isothermal Grüneisen parameter observed[38] for $BaFe_2As_2$ that was treated as a direct effect of the electron-phonon coupling, could disappear by taking the Fe-As volume instead of the total unit cell volume in the definition of the Grüneisen parameter, as shown in our work.

The shift of the 25 meV peak upon doping was observed in Refs. 18 and 21 and explained therein by electron-phonon coupling. In our study we also observe a small shift of this peak upon doping. However, a proportional shift is seen for the 32 meV peak as well. We therefore associate such a shift with the small change of the Fe-As bond length. No anomalies upon doping are seen also for the Sm peak at 22.6 meV. The doping leads to a broadening of this peak, which can be explained by the disorder induced in the SmO layer. However, the peak position shows almost no change.

The low-energy part of the Fe DPS extends up to the 12 meV peak. This acoustic part of the DPS depends on the vibrations in both FeAs and SmO layers, so that the response to the change of the external conditions is different from that for the high energy phonons. In particular, the increase of the rare earth atomic mass from La to Sm leads to the shift of the

12 meV peak even down while Fe-As bond lengths decrease. However, there is no effect of the doping on the position and on the shape of this peak for Fe nor for Sm DPS.

The most interesting behavior of the DPS is observed for the 16 meV peak of the Fe DPS. It shows anomalies in the temperature dependence for both doped and parent compounds. This peak, which has E_g symmetry, corresponds to the vibrations of the Fe atoms in the Fe plane. The anomalies in the behavior across structural phase transition is expected as a splitting into two modes due to the differentiation of the in-plane lattice parameters.[10] Such a splitting was observed by Raman scattering[48] in $BaFe_2As_2$. Therefore, the observed jump of the peak position by ∼0.2 meV across the structural transition can be related to the structural change in the Fe plane.

The doping also leads to the hardening of the 16 meV peak which is mainly seen at low temperature. The enhanced softening of this peak upon heating makes the difference in the position quite small at room temperature. Such softening, in principle, could be explained by the temperature driven structure change. However, such effect was not observed due to volume contraction in the high pressure studies of the parent compounds. The parent and doped compounds here are in the same tetragonal phase and can be compared. The absence of the anomalous behavior of the 16 meV peak in the high pressure studies prove that the observed enhanced softening is not due to the structure changes but has pure temperature origin. It can be related to the renormalization of the force constants due to the adiabatic electron-phonon coupling.[49]

The doping also leads to the increase of the Fe vibrations at ∼20 meV mainly in the Sm compound. This result has to be taken with care, because the reason of such enhancement in the Sm compound could be impurities existing in the doped sample. On the other hand, the presence of this effect also in the Nd compound, where impurities were not observed, suggests the universality of such an effect. Similar increase of the DPS at ∼20 meV upon doping was also observed by inelastic x-ray scattering[19,21] in Nd and Sm compounds. The effect was explained by the shift of the peak position due to the doping.[50] However, according to our measurements the position of the 20 meV peak does not change. The increase of the peak height could be related to the modification of the force constants leading to the enhancing of the amplitude of Fe vibrations near 20 meV.

VI. CONCLUSION

We have performed a systematic study of the density of phonon states in the 1111 family of iron-based superconductors upon rare-earth substitution, doping, application of high pressure, and changing temperature. We found that the positions of most phonon peaks change proportionally to the change of the Fe-As bond length. The change of this parameter explains the change of the Fe density of phonon states above 25 meV. In contrast, anomalies in the behavior of the phonon modes near 16–20 meV were observed upon doping and change in temperature. The F doping leads to a modification of the force constants in the Fe-As layer resulting in the hardening of the 16 meV peak and enhancement of the vibration amplitude of the 20 meV peak of the Fe DPS. In addition, an enhanced softening of the 16 meV peak is observed for the doped compounds indicating strong electron-phonon coupling. This suggests that phonons near this energy play an important role in the competition between superconductivity and magnetism in these materials. Whereas there are several theoretical investigations of the influence of such a coupling to the 20 meV phonon modes, the study of such effect at 16 meV is missing and would be of importance.

ACKNOWLEDGMENTS

The European Synchrotron Radiation Facility is acknowledged for provision of synchrotron radiation beamtime and facility at beamlines ID18 and ID22N. R.H. acknowledges support from the Helmholtz-University Young Investigator Group VH NG-407 “Lattice Dynamic in Emerging Functional Materials.” M.A. acknowledges support from the Helmholtz-University Young Investigator Group VH NG-510 “Complex Ordering Phenomena in Multifunctional Oxides.” Research at ORNL was supported by the US Department of Energy, Basic Energy Sciences, Materials Sciences and Engineering Division.

*ilya.sergeev@desy.de

[1] Y. Kamihara, T. Watanabe, M. Hirano, and H. Hosono, J. Am. Chem. Soc. **130**, 3296 (2008).
[2] K. Ishida, Y. Nakai, and H. Hosono, J. Phys. Soc. Jpn. **78**, 062001 (2009).
[3] J. Paglione and R. L. Greene, Nat. Phys. **6**, 645 (2010).
[4] G. R. Stewart, Rev. Mod. Phys. **83**, 1589 (2011).
[5] A. S. Sefat, Rep. Prog. Phys. **74**, 124502 (2011).
[6] H. Okada, K. Igawa, H. Takahashi, Y. Kamihara, M. Hirano, H. Hosono, K. Matsubayashi, and Y. Uwatoko, J. Phys. Soc. Jpn. **77**, 113712 (2008).
[7] D. A. Zocco, R. E. Baumbach, J. J. Hamlin, M. Janoschek, I. K. Lum, M. A. McGuire, A. S. Sefat, B. C. Sales, R. Jin, D. Mandrus *et al.*, Phys. Rev. B **83**, 094528 (2011).
[8] I. I. Mazin and M. D. Johannes, Nat. Phys. **5**, 141 (2009).
[9] T. Fukuda, A. Q. R. Baron, S. ichi Shamoto, M. Ishikado, H. Nakamura, M. Machida, H. Uchiyama, S. Tsutsui, A. Iyo, H. Kito *et al.*, J. Phys. Soc. Jpn. **77**, 103715 (2008).
[10] T. Yildirim, Physica C **469**, 425 (2009).
[11] L. Boeri, M. Calandra, I. I. Mazin, O. V. Dolgov, and F. Mauri, Phys. Rev. B **82**, 020506 (2010).
[12] Y. Gallais, A. Sacuto, M. Cazayous, P. Cheng, L. Fang, and H. H. Wen, Phys. Rev. B **78**, 132509 (2008).
[13] V. G. Hadjiev, M. N. Iliev, K. Sasmal, Y.-Y. Sun, and C. W. Chu, Phys. Rev. B **77**, 220505 (2008).
[14] C. Marini, C. Mirri, G. Profeta, S. Lupi, D. Di Castro, R. Sopracase, P. Postorino, P. Calvani, A. Perucchi, S. Massidda *et al.*, Europhys. Lett. **84**, 67013 (2008).
[15] L. Zhang, T. Fujita, F. Chen, D. L. Feng, S. Maekawa, and M. W. Chen, Phys. Rev. B **79**, 052507 (2009).

[16]M. Granath, J. Bielecki, J. Holmlund, and L. Börjesson, Phys. Rev. B **79**, 235103 (2009).
[17]L. Zhang, P. F. Guan, D. L. Feng, X. H. Chen, S. S. Xie, and M. W. Chen, J. Am. Chem. Soc. **132**, 15223 (2010).
[18]M. Le Tacon, M. Krisch, A. Bosak, J.-W. G. Bos, and S. Margadonna, Phys. Rev. B **78**, 140505 (2008).
[19]M. Le Tacon, T. R. Forrest, C. Rüegg, A. Bosak, A. C. Walters, R. Mittal, H. M. Rønnow, N. D. Zhigadlo, S. Katrych, J. Karpinski *et al.*, Phys. Rev. B **80**, 220504 (2009).
[20]T. Fukuda, A. Q. R. Baron, H. Nakamura, S. Shamoto, M. Ishikado, M. Machida, H. Uchiyama, A. Iyo, H. Kito, J. Mizuki *et al.*, Phys. Rev. B **84**, 064504 (2011).
[21]M. Le Tacon, T. R. Forrest, Ch. Rüegg, A. Bosak, J. Noffsinger, A. C. Walters, P. Toulemonde, A. Palenzona, N. D. Zhigadlo, J. Karpinski *et al.*, J. Phys. Chem. Solids **72**, 523 (2011).
[22]Y. Qiu, M. Kofu, W. Bao, S.-H. Lee, Q. Huang, T. Yildirim, J. R. D. Copley, J. W. Lynn, T. Wu, G. Wu *et al.*, Phys. Rev. B **78**, 052508 (2008).
[23]A. D. Christianson, M. D. Lumsden, O. Delaire, M. B. Stone, D. L. Abernathy, M. A. McGuire, A. S. Sefat, R. Jin, B. C. Sales, D. Mandrus *et al.*, Phys. Rev. Lett. **101**, 157004 (2008).
[24]M. Zbiri, R. Mittal, S. Rols, Y. Su, Y. Xiao, H. Schober, S. L. Chaplot, M. R. Johnson, T. Chatterji, Y. Inoue *et al.*, J. Phys.: Condens. Matter **22**, 315701 (2010).
[25]S. Higashitaniguchi, M. Seto, S. Kitao, Y. Kobayashi, M. Saito, R. Masuda, T. Mitsui, Y. Yoda, Y. Kamihara, M. Hirano *et al.*, Phys. Rev. B **78**, 174507 (2008).
[26]A. S. Sefat, M. A. McGuire, B. C. Sales, R. Jin, J. Y. Howe, and D. Mandrus, Phys. Rev. B **77**, 174503 (2008).
[27]M. A. McGuire, A. D. Christianson, A. S. Sefat, B. C. Sales, M. D. Lumsden, R. Jin, E. A. Payzant, D. Mandrus, Y. Luan, V. Keppens *et al.*, Phys. Rev. B **78**, 094517 (2008).
[28]M. A. McGuire, R. P. Hermann, A. S. Sefat, B. C. Sales, R. Jin, D. Mandrus, F. Grandjean, and G. J. Long, New J. Phys. **11**, 025011 (2009).
[29]J. Rodríguez-Carvajal, Physica B: Condens. Matter **192**, 55 (1993).
[30]F. Nitsche, A. Jesche, E. Hieckmann, T. Doert, and M. Ruck, Phys. Rev. B **82**, 134514 (2010).
[31]S. Margadonna, Y. Takabayashi, M. T. McDonald, M. Brunelli, G. Wu, R. H. Liu, X. H. Chen, and K. Prassides, Phys. Rev. B **79**, 014503 (2009).
[32]R. Rüffer and A. I. Chumakov, Hyperfine Interact. **97-98**, 589 (1996).
[33]I. Sergueev, H. Wille, R. P. Hermann, D. Bessas, Y. V. Shvyd'ko, M. Zajac, and R. Rüffer, J. Synchrotron Radiat. **18**, 111 (2011).
[34]A. Barla, J. P. Sanchez, Y. Haga, G. Lapertot, B. P. Doyle, O. Leupold, R. Rüffer, M. M. Abd-Elmeguid, R. Lengsdorf, and J. Flouquet, Phys. Rev. Lett. **92**, 066401 (2004).
[35]H. Giefers, R. Lubbers, K. Rupprecht, G. Wortmann, D. Alfe, and A. Chumakov, High Press. Res. **22**, 501 (2002).
[36]V. Kohn and A. Chumakov, Hyperfine Interact. **125**, 205 (2000).
[37]A. I. Chumakov, R. Rüffer, O. Leupold, and I. Sergueev, Structural Chemistry **14**, 109 (2003).
[38]O. Delaire, M. S. Lucas, A. M. dos Santos, A. Subedi, A. S. Sefat, M. A. McGuire, L. Mauger, J. A. Muñoz, C. A. Tulk, Y. Xiao *et al.*, Phys. Rev. B **81**, 094504 (2010).
[39]S. Tsutsui, C.-H. Lee, C. Tassel, Y. Yoshida, Y. Yoda, K. Kihou, A. Iyo, and H. Eisaki, J. Phys. Soc. Jpn. **79**, 013706 (2010).
[40]H. Kobayashi, S. Ikeda, Y. Yoda, H. Nakamura, and M. Machida, Phys. Rev. B **84**, 184304 (2011).
[41]H. Takahashi, H. Okada, K. Igawa, K. Arii, Y. Kamihara, S. Matsuishi, M. Hirano, H. Hosono, K. Matsubayashi, and Y. Uwatoko, J. Phys. Soc. Jpn. **77**, 78 (2008).
[42]J. Zhao, L. Wang, D. Dong, Z. Liu, H. Liu, G. Chen, D. Wu, J. Luo, N. Wang, Y. Yu *et al.*, J. Am. Chem. Soc. **130**, 13828 (2008).
[43]M. Calamiotou, D. Lampakis, E. Siranidi, J. Karpinski, N. D. Zhigadlo, and E. Liarokapis, Physica C **483**, 136 (2012).
[44]V. Ksenofontov, G. Wortmann, A. I. Chumakov, T. Gasi, S. Medvedev, T. M. McQueen, R. J. Cava, and C. Felser, Phys. Rev. B **81**, 184510 (2010).
[45]G. Garbarino, P. Toulemonde, M. Álvarez-Murga, A. Sow, M. Mezouar, and M. Núñez-Regueiro, Phys. Rev. B **78**, 100507 (2008).
[46]R. Mittal, S. K. Mishra, S. L. Chaplot, S. V. Ovsyannikov, E. Greenberg, D. M. Trots, L. Dubrovinsky, Y. Su, T. Brueckel, S. Matsuishi *et al.*, Phys. Rev. B **83**, 054503 (2011).
[47]F. Yndurain, Europhys. Lett. **94**, 37001 (2011).
[48]L. Chauvière, Y. Gallais, M. Cazayous, A. Sacuto, M. A. Méasson, D. Colson, and A. Forget, Phys. Rev. B **80**, 094504 (2009).
[49]O. Delaire, K. Marty, M. B. Stone, P. R. C. Kent, M. S. Lucas, D. L. Abernathy, D. Mandrus, and B. C. Sales, Proc. Natl. Acad. Sci. **108**, 4725 (2011).
[50]J. Noffsinger, F. Giustino, S. G. Louie, and M. L. Cohen, Phys. Rev. Lett. **102**, 147003 (2009).